Erschienen in: Molecular Therapy - Nucleic Acids ; 5 (2016), 2. - e286
https://dx.doi.org/10.1038/mtna.2015.59

Citation: Molecular Therapy—Nucleic Acids (2016) 5, e286; doi:10.1038/mtna.2015.59
Official journal of the American Society of Gene & Cell Therapy

www.nature.com/mtna

Endocytosis and Endosomal Trafficking of DNA After Gene Electrotransfer *In Vitro*

Christelle Rosazza[1–3], Hendrik Deschout[4], Annette Buntz[1], Kevin Braeckmans[4], Marie-Pierre Rols[2,3] and Andreas Zumbusch[1]

DNA electrotransfer is a successful technique for gene delivery into cells and represents an attractive alternative to virus-based methods for clinical applications including gene therapy and DNA vaccination. However, little is currently known about the mechanisms governing DNA internalization and its fate inside cells. The objectives of this work were to investigate the role of endocytosis and to quantify the contribution of different routes of cellular trafficking during DNA electrotransfer. To pursue these objectives, we performed flow cytometry and single-particle fluorescence microscopy experiments using inhibitors of endocytosis and endosomal markers. Our results show that ~50% of DNA is internalized by caveolin/raft-mediated endocytosis, 25% by clathrin-mediated endocytosis, and 25% by macropinocytosis. During active transport, DNA is routed through multiple endosomal compartments with, in the hour following electrotransfer, 70% found in Rab5 structures, 50% in Rab11-containing organelles and 30% in Rab9 compartments. Later, 60% of DNA colocalizes with Lamp1 vesicles. Because these molecular markers can overlap while following organelles through several steps of trafficking, the percentages do not sum up to 100%. We conclude that electrotransferred DNA uses the classical endosomal trafficking pathways. Our results are important for a generalized understanding of gene electrotransfer, which is crucial for its safe use in clinics.

Molecular Therapy—Nucleic Acids (2016) **5**, e286; doi:10.1038/mtna.2015.59; published online 9 February 2016
Subject Category: Nucleic acid chemistries

Introduction

Electroporation is a safe and efficient method of molecule delivery into cells and tissues. The application of an external electric field drastically increases plasma membrane permeability to nonpermeant molecules such as hydrophilic compounds and plasmid DNA. This method is currently used in clinics, where it is termed electrochemotherapy, for local delivery of antitumor drugs including bleomycin and cisplatin, which are given direct access to the cytosol.[1–3] *In vivo* electroporation is also a promising method of gene delivery that can be used for cancer gene therapy and DNA vaccination.[4–8]

The physicochemical structures driving the permeability of plasma membranes after electroporation are thought to result from the reorganization of lipids into pores. Although these membrane defects are predicted to be stable for several minutes and to be large enough to allow DNA passage,[9] DNA instead accumulates at the membrane and remains stationary for ~10 minutes.[10] DNA forms clusters of 100–500 nm in diameter that are inserted into the membrane, where they are immobile and rapidly protected against degradation from extracellular nucleases. This observation suggests that DNA might be enclosed in membranous structures.[11]

DNA internalization occurs after membrane resealing and involves the passage of large DNA aggregates. One possible scenario is that an endocytosis-like process takes place, as is the case for many viral or chemical vectors. The shape, lifetime, size, stability, and resistance to degradation of DNA complexes at the membrane are consistent with its engulfment into vesicles. Electroporation-induced endocytosis has been hypothesized for the delivery of proteins.[12–15] The possibility that endocytosis participates in DNA electrotransfer has started to emerge,[16–20] but the generality of this mechanism for DNA translocation across membranes is not yet a standard concept in the literature.

Once inside the cytoplasm, DNA clusters observed at the membrane retain a patch-like appearance until their arrival at the vicinity of the nucleus.[10,21] We have shown, via single particle tracking experiments (SPT), that DNA aggregates are actively transported by the actin and the microtubule networks.[21] The motion of DNA in the cytoplasm is similar to that described for endosomes: DNA aggregates have phases of long-range and bidirectional transport interrupted by phases of diffusion. DNA kinetics were also found to be similar to those of endosomes. However, single-particle tracking experiments alone do not shed light onto the question whether the aggregates are transported inside vesicles or as naked DNA (interacting with adapter proteins).

The work presented here aims to unravel the different endocytic pathways and the subsequent intracellular trafficking of electrotransferred DNA. Most current methods for studying internalization of particles involve either exclusion of specific endocytic mechanisms, using inhibitors of endocytosis and mutant cell lines, or colocalization of particles with endocytic markers. The main limitation of these methods is that neither chemical inhibitors nor endocytic markers are completely

[1]Department of Chemistry, University of Konstanz, Konstanz, Germany; [2]Department of Structural Biology and Biophysics, Institute of Pharmacology and Structural Biology (IPBS), CNRS UMR5089, Toulouse, France; [3]University of Toulouse III, UPS, Toulouse, France; [4]Laboratory of General Biochemistry and Physical Pharmacy, Department of Pharmaceutics, University of Ghent, Ghent, Belgium Correspondence: Andreas Zumbusch, Department of Chemistry, Universität Konstanz, Universitätstrasse 10, D-78457 Konstanz, Germany. E-mail: andreas.zumbusch@uni-konstanz.de
Keywords: colocalization; electric field; electroporation; endocytosis; endosomal trafficking; gene electrotransfer; plasmid DNA; single-particle tracking
Received 18 December 2015; accepted 18 December 2015; published online 9 February 2016. doi:10.1038/mtna.2015.59

specific. Indeed, inhibitors can disturb multiple endocytic pathways, and markers can utilize several different endocytic mechanisms. A more comprehensive tactic, which we also employed here, utilizes cells transfected with constructs containing GFP-fusion to proteins that reside in specific endocytic vesicles or intracellular organelles. In a first set of experiments, we measured the effect of different endocytic inhibitors on gene expression in Chinese Hamster Ovary (CHO) cells using flow cytometry. To better discriminate the various endocytic pathways contributing to DNA internalization, two to three inhibitors per pathway were chosen and several concentrations tested. Secondly, static colocalization analyses were conducted in living CHO cells to quantitatively determine the proportion of DNA aggregates colocalizing with three endocytosis markers (transferrin (Tf), cholera toxin B (CTB), and 70-kDa dextran). Finally, we performed correlation analyses between DNA and several endosomal membrane markers (Rab5, Rab9, Rab11, and Lamp1 tagged with enhanced green fluorescent protein (EGFP)). Dual-color single-particle tracking was performed to monitor the dynamics of endocytosis and to quantify the correlation of DNA trajectories with those of specific trafficking markers.

Results

Endocytosis of electrotransferred DNA leads to gene expression

In order to evaluate whether endocytosis is an important process leading to the internalization of DNA after electroporation, we performed EGFP reporter gene expression in CHO cells that were treated with different endocytic inhibitors. Both the percentage of fluorescent cells (*i.e.*, transfection efficiency) and their mean fluorescence intensity (*i.e.*, the transfection level) were measured using flow cytometry. Since the pathway specificity of the inhibitors is only partial, two drugs per main pathway were used and three to four concentrations were tested.

We assessed seven endocytosis inhibitors in total: Wortmannin (Wort) and ethyl-isopropyl-amiloride (EIPA) affect macropinocytosis,[22] chlorpromazine (CPZ) and monodansylcadaverine (MDC) are inhibitors of the clathrin-mediated pathway, and filipin (Fil) and genistein (Gen) inhibit caveolin/raft-mediated endocytosis. Methyl-beta-cyclodextrin (MβCD), which primarily disrupts caveolin/raft-mediated endocytosis via cholesterol depletion, can also interfere with macropinocytosis and clathrin-mediated endocytosis. All measurements were normalized to control cells (transfected but untreated) in which the population percentage of reporter expression was 37%, and the mean fluorescence intensity was 2,415 AU. Each endocytic inhibitor reduced both the transfection efficiency and level (**Figure 1**) with good correlation between drug concentration and inhibition of the reporter expression. In detail, the following results were obtained.

Highly significant declines in gene expression were measured for any drug concentration of MβCD: relative to control cells, fewer than half of treated cells expressed the EGFP reporter protein (37% at 5 µmol/l MβCD, **Figure 1a**), and among those, the transfection level fell to 50% (**Figure 1b**). From these results, we infer that the higher the degree of cholesterol depletion, the more severe the decreases in transfection efficiency and subsequent expression of internalized DNA.

After Wort treatment, we observed a strongly dose-dependent and a highly significant reduction in the percentage of cells expressing EGFP (from 85 to 65% of the control, **Figure 1a**). The two lowest Wort concentrations did not significantly alter transfection level, while the two highest tested concentrations efficiently diminished DNA expression (85 and 65% relative to control cells, respectively, **Figure 1b**). The percentage of EGFP-positive cells was greatly decreased by any drug concentration of EIPA, giving between 65 and 70% of the control expression (**Figure 1a**). EIPA treatment's effect on the quantity of EGFP expressed was less obvious and amounted to 85–90% of the control (**Figure 1b**), with only one difference found to be statistically significant.

CPZ-induced decrease in gene expression was highly significant and proportional to the amount of drug added in the medium. For the higher concentrations, only 60% of the cells were found to express EGFP (**Figure 1a**) and among them, the expression level reached only 55–80% of the control cells (**Figure 1b**). The largest concentrations of MDC reduced the percentage of EGFP-positive cells to 70% (**Figure 1a**) and the average fluorescence intensity to 80% relative to the control population (**Figure 1b**).

The least inhibitory drug was Fil for which most tested concentrations induced changes in gene expression that were not statistically significant. However, the highest concentration of Fil lowered the transfection efficiency and level to 80 and 70%, respectively. Treatment with Gen was very effective in reducing the percentage of cells exhibiting EGFP signal (40–60% of the control cells, **Figure 1a**), with a strong dependence on the drug concentration. Among these cells, the amount of expressed EGFP ranged from unchanged to 60% relative to the control (**Figure 1b**).

Electrotransferred DNA colocalizes with endocytic markers

As a second independent test for the involvement of endocytosis in DNA electrotransfer, we performed colocalization experiments between DNA and three endocytic markers. We used labeled Tf to assess clathrin-mediated endocytosis, CTB to evaluate caveolin/raft-mediated endocytosis, and 70-kDa dextran to highlight fluid-phase endocytosis, which includes macropinocytosis and any endocytic process that engulfs large amounts of extracellular medium (*e.g.*, glycophosphatidylinositol (GPI)-enriched endocytic compartments (GEECs)). Images were sequentially recorded using a wide-field microscope with single-molecule sensitivity.[21] For the quantification, we used an object-based method[23,24] in which colocalization is defined by a spatial overlap between an object of the first channel and the center position of an object of the second channel. Our results indicated that DNA partially colocalized with all endocytic markers (**Figures 2** and **3**). Clathrin-mediated endocytosis was implicated in DNA uptake as DNA colocalized with Tf at 25 ± 6% (**Figures 2a** and **3**). CTB and DNA colocalized at 48 ± 8%, which indicates entry via raft-mediated pathways that can include caveolae or noncaveolae (**Figures 2b** and **3**). 70-kDa dextran also colocalized with DNA, at a rate of 30 ± 4%, which can be interpreted as a contribution of

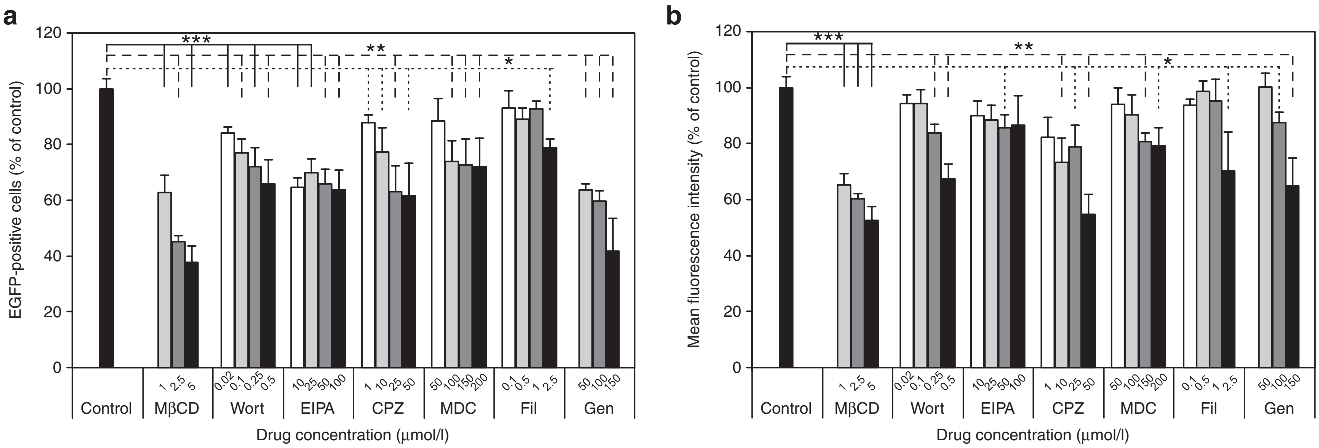

Figure 1 Gene expression in CHO cells after treatment with different endocytic inhibitors. EGFP reporter gene expression was measured using flow cytometry 24 hours after separate treatment of CHO cells with different concentrations of methyl-beta-cyclodextrin (MβCD), wortmannin (Wort), ethyl-isopropyl-amiloride (EIPA), chlorpromazine (CPZ), monodansylcadaverine (MDC), filipin (Fil), and genistein (Gen). Incubations were performed 1 hour before the application of the electric field (10 pulses at 0.4 kV/cm, 5 ms and 1 Hz) in the presence of pEGFP-C1 plasmid DNA. (**a**) Percentage of fluorescent cells (transfection efficiency) and (**b**) mean fluorescence intensity (transfection level) (mean + SEM, $n = 5$–7). Controls represent transfected, but otherwise untreated cells. $^*P < 0.05$ (dotted line), $^{**}P < 0.01$ (dashed line), $^{***}P < 0.001$ (solid line)

macropinocytosis and GPI-enriched endocytic compartments to DNA internalization (**Figures 2c** and **3**). The size of dextran was selected to ensure that its entry mainly occurred through large endosomes. Under our conditions, 70-kDa dextran only weakly colocalized with Tf- or CTB-labeled structures (**Supplementary Figure S1**).

Electrotransferred DNA colocalizes with endosomal markers

In a third line of experiments, we performed a correlation analysis between the motion of different endosomal markers and DNA aggregates. The bases for these experiments are videos of labeled DNA and the respective endosomal marker events, which were recorded at nearly the same time. Correlated movement of DNA and an endosomal marker is a strong indication for DNA transport in a specific class of cellular vesicles.[25] Thus, in contrast to methods primarily used in the literature to date, these experiments make it possible to address the question whether DNA remains enclosed within endocytic vesicles while trafficking in the cytoplasm.

CHO cells were separately transfected with plasmids encoding the EGFP-tagged proteins Rab5, Rab9, Rab11, and Lamp1, which are known respectively to identify early endosomes, late endosomes, recycling endosomes, and lysosomes.[26] The fluorescent signals of both channels were sequentially recorded as time series with a temporal delay of 200 ms between acquisitions for each channel. From the videos, trajectories of the fluorescent particles were generated, and the correlation between the trajectories was calculated using an established algorithm.[25] When the spatiotemporal correlation between all consecutive steps of the trajectories exceeded a certain threshold value, the motion of the corresponding objects was considered to be correlated (**Figure 4a**).

As noted above, correlation of movement is a potent indicator for localization of DNA and an endosomal marker in the same vesicle. However, intracellular motion of vesicles involves not only continuous directional movement but also periods of diffusive motion.[21] During the latter, vesicles move very little and appear nearly immobile (**Figure 4b**), which does not permit correlation analysis to be carried out. Instead, we performed a static object-based colocalization analysis for these trajectories. The mean position of the trajectories in both channels was calculated, and when the distance between these mean positions was below the optical resolution, trajectories were qualified as colocalized. As a result, the analysis yielded a percentage of correlated objects, *i.e.*, objects which undergo correlated motion, and of colocalized objects, *i.e.*, quasi-immobile structures which colocalize.

Microscopy data show that DNA partially colocalized with all endosomal markers (Rab5, Rab11, Rab9, and Lamp1) (**Figure 5**). In order to properly represent the total amount of DNA residing in the vesicles, each bar of the histogram depicted in **Figure 6** summarizes the percentage obtained for both the correlated and colocalized trajectories. For the three Rab proteins, acquisitions were started ~15 minutes after DNA electrotransfer and were performed for up to 1.5 hours. DNA correlation and colocalization with Rab5 were the highest with 38 ± 4% and 32 ± 2%, respectively (**Figures 5a** and **6**). In Rab11-expressing cells, DNA correlated with this endosomal marker at 33 ± 5%, and colocalized at 17 ± 3% (**Figures 5b** and **6**). Between trajectories of Rab9-containing structures and DNA, we found a correlation of 21 ± 5% and a colocalization of 11 ± 4% (**Figures 5c** and **6**). For the Lamp1 experiments, acquisitions were started ~1 hour after DNA electrotransfer and were performed for up to 1 hour. Correlation of DNA with Lamp1-marked membranes was calculated to be 41 ± 6% and colocalization to be 19 ± 4% (**Figures 5d** and **6**).

Discussion

DNA electrotransfer is an easy and efficient method of gene delivery and an attractive alternative to virus-based methods for clinical applications such as gene therapy and DNA vaccination. Nonetheless, the processes leading to internalization of DNA and its fate inside cells are poorly understood. Endocytosis has received little consideration as a possible mechanism by which DNA could cross the plasma membrane. This was due to the absence of known cellular receptors for DNA, and because electric fields were shown to permeabilize plasma membranes, presumably by creating pores large enough to allow direct access to the cytoplasm. Electropermeabilization of the plasma membrane remains a crucial step for gene delivery, but internalization of DNA via electropores is not easy to envision as, unlike small molecules, DNA forms distinct, stable, and large clusters at the cell membrane prior to its passage into the cytoplasm. The objectives of this work were twofold. We first sought to establish that endocytosis is important for DNA electrotransfer and to quantify different endocytic pathways' contributions to DNA internalization. This information is central not only for our basic knowledge of DNA passage across plasma membranes but also for optimizing gene delivery using electrotransfer methods. Secondly, we aimed to quantify the pattern with which engulfed DNA travels through cytoplasmic trafficking organelles. Knowledge of the DNA distribution among endosomal compartments provides critical insights into the transfection efficiency achievable with DNA electrotransfer, as it indicates the relative quantities of DNA that can potentially reach the nucleus or be lost in degradation pathways.

Clathrin-mediated endocytosis of DNA

Clathrin-mediated endocytosis is perhaps least suspected to participate in DNA electrotransfer, since DNA has no known receptors on cell membranes. Nevertheless, our work here shows that it is partly involved in DNA internalization after electroporation. The percentage of cells expressing transfected DNA and their mean expression level were significantly decreased by treatment with both CPZ and MDC, the latter of which appears to be a relatively specific blocker of clathrin-mediated internalization.[22] All but the lowest tested MDC concentration led to identical inhibition of the transfection efficiency, which suggests that blockage of the pathway was complete, and that clathrin-mediated endocytosis represents ~30% of the internalization routes taken by electrotransferred DNA. CPZ inhibits clathrin-mediated endocytosis of various plasma membrane proteins, and there is no evidence in the literature that CPZ affects caveolin/raft-mediated endocytosis.[27–29] This drug may, however, interfere with the biogenesis of large vesicles such as macropinosomes,[22] which could explain the observed difference in expression efficiencies between cells treated with CPZ in comparison with MDC.

Earlier studies revealed that MβCD treatment almost completely eliminates endocytosis of Tf, EGF, and lipoplexes by inhibiting the invagination of clathrin-coated pits.[30–32] However, these results were observed at very high MβCD concentrations (mmol/l range). We have used comparatively low MβCD concentrations (1–5 μmol/l) which likely contributed to a more moderate inhibition of the clathrin-mediated pathway. Our analysis of colocalization between DNA and the endocytosis marker Tf also supports the conclusion that electrotransferred DNA is internalized via the clathrin-mediated endocytosis. Quantification established a 25% colocalization which is in good agreement with the results obtained in our drug treatment and gene expression experiments.

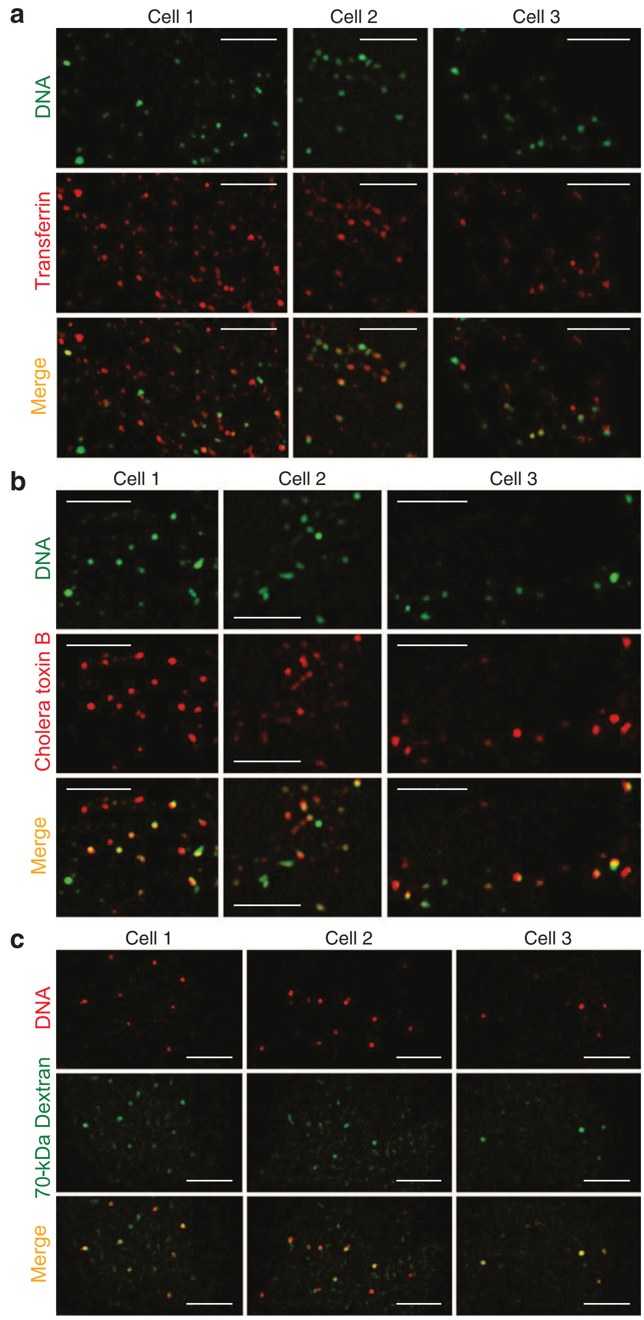

Figure 2 Colocalization of DNA with several endocytic markers. Transferrin highlights the involvement of clathrin-mediated endocytosis, cholera toxin B the participation of caveolin/raft-mediated endocytosis, and 70-kDa dextran the contribution of fluid-phase endocytosis. DNA was electrotransferred into CHO cells via the application of 10 electric pulses of 5 ms at 1 Hz and 0.4 kV/cm. Images were taken sequentially using wide-field microscopy. (**a**) Cy3-DNA (green), Alexa fluor 647-transferrin (red) and merge of the two channels, (**b**) Cy3-DNA (green), Alexa fluor 647-cholera toxin B (red) and merge of the two images, and (**c**) Cy5-DNA (red), rhodamine-(70-kDa)-dextran (green), and merge of the two channels. **a–c**, Bar = 5 μm.

Our results are further supported by complementary evidence from the literature[17,18] including our previous findings that actin undergoes bursts of polymerization where DNA–membrane interactions occur, and that drug-mediated disruption of the actin network diminishes DNA interaction with the membrane and reporter expression.[19,21] Furthermore, Wu and Yuan[17] report a drastic reduction of DNA expression after incubation with dynasore, an inhibitor of dynamin. Dynamin and the actin network are both crucial for numerous endocytic pathways including clathrin-mediated endocytosis.[33]

Caveolin/raft-mediated endocytosis of DNA

Caveolin- and raft-mediated endocytosis represent a large subset of pathways that share common features among which is a strict requirement for cholesterol.[34] This makes it very difficult to define good tools for the investigation of their independent contributions to endocytosis. Cholesterol-sensitive internalization of lipid rafts can be classified into three major pathways including dynamin-dependent endocytosis of caveolae or noncaveolar vesicular carriers (IL-2), dynamin-independent endocytosis via noncaveolar tubular intermediates (GEECs), and dynamin-independent endocytosis of nontubular carriers (flotillin, Arf6).[34,35] The depletion of cholesterol by MβCD and Fil has been shown to disrupt the composition of lipid rafts which are therefore unable to localize and segregate proteins and thus to perform endocytosis.[36] All of these pathways are also Gen- and actin dynamic-sensitive.[37]

In our experiments, MβCD affected DNA expression the most drastically with clear dose dependence. Gen treatment also strongly impaired gene expression. If one assumes complete inhibition by our treatments, our observations indicate that 50–60% of DNA internalization is mediated by rafts. Gen has been shown to inhibit recruitment of dynamin at the surface of vesicles containing SV40,[38] which could indicate that nonclathrin, but dynamin-dependent endocytosis would be more affected by treatment with Gen (caveolae and IL-2 pathways).

By contrast, inhibitions observed after treatment with Fil, which sequesters cholesterol, were not as pronounced. Fil shows good specificity to raft-mediated endocytosis, however, for the internalization of albumin, it can also greatly inhibit degradation in the multivesicular bodies.[39] If less degradation occurs as well for electrotransferred DNA, more DNA should be available for efficient targeting of the nucleus and expression, which could account for the less drastic effect of Fil in comparison with MβCD and Gen.

An earlier study demonstrated that although the internalization of adeno-associated virus is clearly mediated by the GEEC pathway, it remains sensitive to EIPA.[40] Therefore, EIPA appears to be also a GEEC endocytosis inhibitor. Consequently, a part of the observed diminution in the transfection efficiency after EIPA treatment could be attributed to the involvement of the GEEC pathway in the internalization of electrotransferred DNA.

The lack of specific pharmacological inhibitors is not the only obstacle in discriminating the different raft-mediated endocytosis routes. The predominant raft marker CTB also has low specificity, as it has been implicated in caveolar,[41–45] noncaveolar,[46,47] flotillin-dependent[48] and the dynamin-independent GEEC pathway.[46] Our colocalization study between DNA and CTB revealed about 50% of shared subcellular structures, which probably reflects the contributions of several of the raft-mediated pathways (caveolin, flotillin, GEEC, IL-2, and Arf6) to DNA internalization.

As noted in the previous section, there is strong evidence for the participation of actin and dynamin during DNA internalization,[17,19,21] which additionally implicates the involvement of raft-mediated endocytosis. Recent work has demonstrated long-lasting inhibition of DNA electrotransfer in mouse

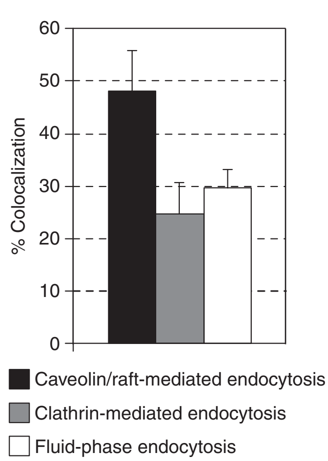

Figure 3 Quantification of the colocalization of DNA with three different endocytic markers. Quantification was performed using the overlap approach.[24] The analysis of more than 100 cells with each endocytic marker gave the percentages shown in the graph.

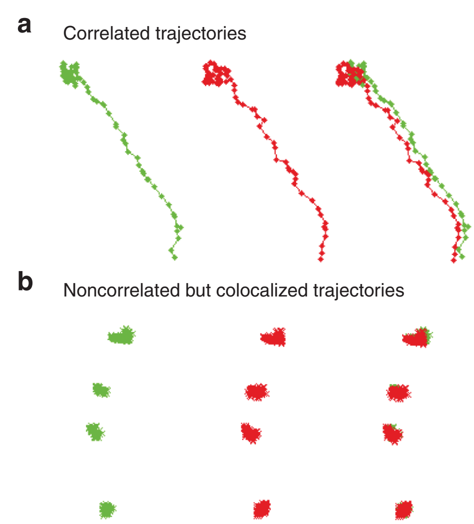

Figure 4 Examples of trajectories visualized through the analysis program. Trajectories in green represent endosomal proteins fused with EGFP, and trajectories in red correspond to Cy5-labeled DNA. (**a**) Rab5 and DNA trajectories exhibited long-range active transport, and their motions are correlated. (**b**) Lamp1 and DNA trajectories did not correlate, most likely due to the diffusion mode of motion. Assuming DNA inside the vesicle and the Lamp1/Rab protein into the membrane, each particle has a certain degree of freedom that superimposes with the inherent noncorrelation of random walks. However, these trajectories were detected as colocalized.

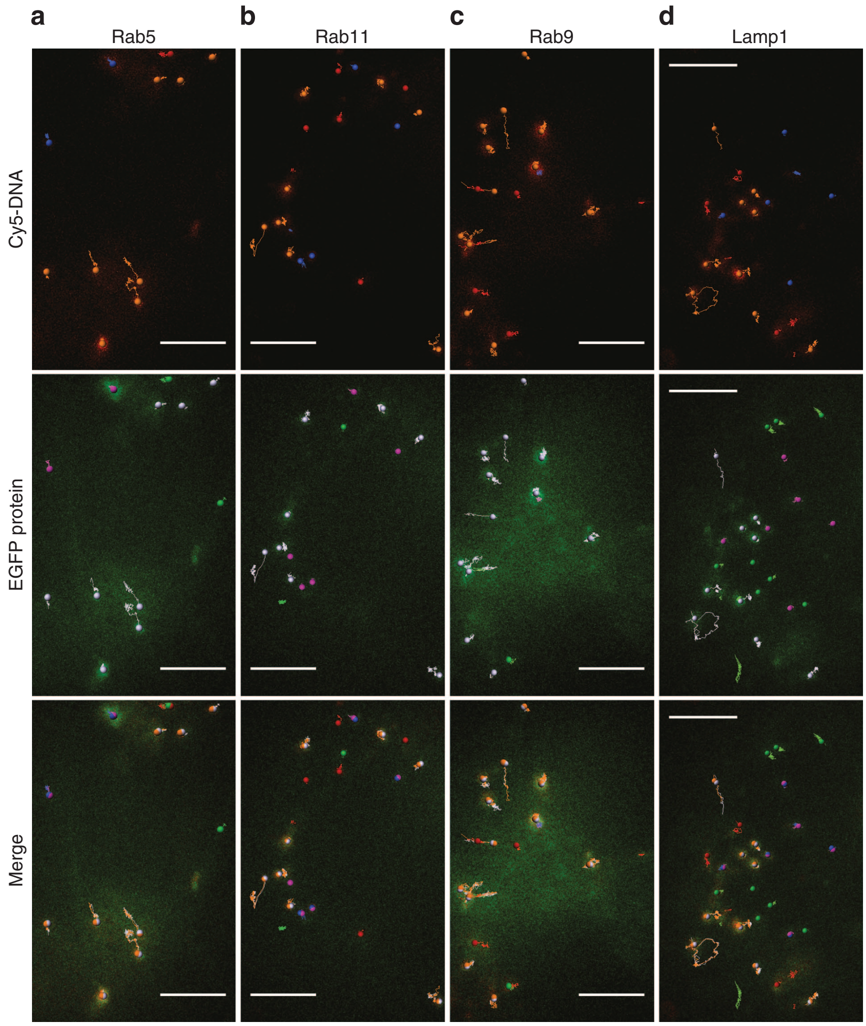

Figure 5 Dual-color SPT of DNA and endosomal proteins in CHO cells after electroporation. Cy5-labeled DNA was electrotransferred into CHO cells separately expressing EGFP-Rab5, Rab11, Rab9, and Lamp1 plasmid constructs. Using a wide-field microscope, time series were recorded sequentially with a delay of 200 ms between the two channels. Using dual-color SPT, we visualized the respective movements of the objects. Correlated trajectories are highlighted in orange (DNA) and light purple (EGFP-markers), colocalized trajectories are drawn in blue (DNA) and pink (EGFP-markers) and the noncorrelated and noncolocalized trajectories are in red (DNA) and green (EGFP-markers). (**a**) DNA in early endosomes (Rab5), (**b**) DNA in recycling endosomes (Rab11), (**c**) DNA in late endosomes (Rab9), and (**d**) DNA in lysosomes (Lamp1). **a–d**, Bar = 5 µm

muscle after MβCD treatment, which intimates that *in vivo* administration of MβCD yields comparable results to those described in the present study.[18]

Macropinocytosis of DNA

The first indication for induction of macropinocytosis in electroporated cells derived from observations of electric field induced ruffling and blebbing of the plasma membrane.[12,13,49] Studies exploring the electrotransfer of proteins into cells also suggested a macropinocytosis-related mechanism of internalization.[12,13,50] The work presented here suggests that electrotransfer of plasmid DNA partially relies on the same principles.

Wort and EIPA both significantly decreased DNA transfection efficiency, with Wort showing a clear dose dependence. EIPA has been used as the main diagnostic test to identify macropinocytosis, since it inhibits Na^+/H^+ exchangers that are very important for this endocytic process.[51–53] The inhibitory effect of EIPA in our experiments was not dose dependent for either transfection efficiency or level, which can indicate that all macropinocytosis events were suppressed and that this pathway accounts for 30–35% of the total amount of DNA engulfed inside cells. It is important to note, though, that because EIPA might also inhibit the GEEC pathway,[40] part of the decrease in DNA expression we observed following EIPA treatment could instead be related to raft-dependent GEEC endocytosis.

Wort inhibits phosphoinositide 3-kinases, which are responsible for the formation of lipid microdomains in membrane ruffles and the dynamics of the macropinocytic cups.[54] A previous study has shown that 70-kDa dextran labels predominantly macropinosomes in control cells, and that Wort treatment eliminates endocytosis of 70-kDa dextran.[54] Smaller probes (3-kDa dextran or lucifer yellow), on the other hand, could label both macro- and micropinosomes of control cells, and after Wort treatment, only small vesicles were labeled. Therefore, the decrease in uptake of fluid-phase probes by inhibitor-treated cells reflects a selective effect of Wort on macropinocytosis and reciprocally the strong selectivity of 70-kDa dextran for probing this pathway. As for EIPA, the highest concentration of Wort we used yielded DNA expression efficiency of 65% relative to the control cells, indicating that macropinocytosis would represent 35% of the internalization routes of electrotransferred DNA. Our second line of experiments yielded 30% of colocalization between DNA and 70-kDa dextran, which agrees well with the percentage estimated from our inhibition experiments. Nonetheless, the calculated percentage was probably slightly overestimated since the GEEC pathway involves the formation of large vesicles as well, which could also engulf 70-kDa dextran. This possibility is supported by our observations of partial colocalization between 70-kDa dextran and CTB that occurred mainly in large vesicles (**Supplementary Figure S1**).

Our work, together with previous studies, shows that DNA electrotransfer fulfills many of the conditions defining macropinocytosis:[55] electroporation induces membrane ruffles and blebbing,[12,13,49] electrotransferred DNA colocalizes with the fluid-phase marker 70-kDa dextran, and gene expression is significantly reduced by inhibition of PI3K (Wort), Na^+/H^+ exchangers (EIPA), actin and microtubules dynamics (latrunculin B, jasplakinolide, nocodazole, and taxol),[19,21] and dynamin (dynasore and perhaps Gen).[17] In addition, the decrease in gene expression associated with MβCD treatment can partially reflect the contribution of macropinocytosis, because MβCD can interfere with both the formation of membrane ruffles and macropinosomes at the plasma membrane.[55,56] Based on our analysis, we conclude that macropinosomes represent about 25% of the DNA aggregates visible in cells.

DNA aggregates are routed to the endosomal trafficking

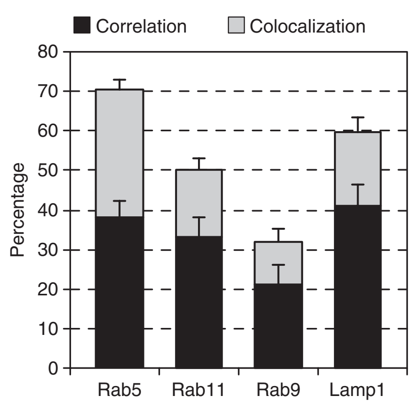

Figure 6 Quantification of the correlation and colocalization between DNA aggregates and endosomal membranes in CHO cells. Cy5-labeled DNA was electrotransferred into CHO cells separately expressing EGFP-Rab5, Rab11, Rab9, and Lamp1 plasmid constructs. After dual-color time lapse recording and SPT analysis, trajectories were tested for correlation and colocalization. The stacked histogram shows the percentage of DNA trajectories that correlated (black) or colocalized (gray) with the trajectories of the mentioned proteins.

DNA was found in significant amounts in all four types of vesicles that we have assessed, namely in early, late, and recycling endosomes, and in lysosomes. These results indicate that DNA is engulfed into vesicles during its transport through the cytoplasm and that it follows the classical intracellular trafficking routes.[26,57] One should note that endosomal trafficking comprises a continuum of vesicles shuttling between compartments. Although the utilized molecular markers undoubtedly distinguish these compartments, they can also partially and transiently overlap.[58]

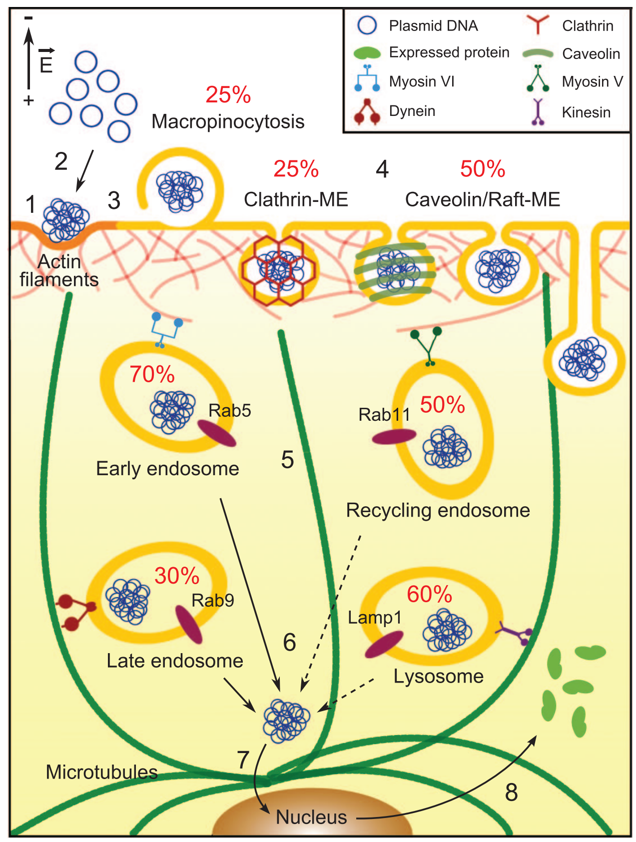

Figure 7 Schematic representation of the mechanism of DNA electrotransfer. During the application of the electric field, (**1**) the plasma membrane is permeabilized (orange), (**2**) DNA is electrophoretically pushed onto the cell membrane side facing the cathode, which results in (**3**) DNA/membrane interactions. DNA aggregates are inserted into the membrane and remain there for about 10 minutes. After the application of the electric field and resealing of the membrane (yellow), (**4**) DNA is internalized by endocytosis with the following approximate contributions: 50% caveolin/raft-mediated endocytosis (caveolin/raft-ME), 25% macropinocytosis, and 25% clathrin-mediated endocytosis (clathrin-ME). (**5**) While being actively transported in the cytoplasm, DNA aggregates pass through the different endosomal compartments. Between 15 minutes and about 1.5 hours after the application of the electric field, on average, 70% of the DNA aggregates are in early endosomes, 50% in recycling endosomes, and 30% in late endosomes. Between 1 and 2 hours after DNA electrotransfer, 60% of the DNA aggregates are in lysosomes. For gene expression to occur, (**6**) DNA must escape from endosomal compartments. This most likely occurs from early or late endosomes (solid line arrow) but it may also be possible from recycling endosomes and lysosomes (dashed line arrow).[58,59] Once in the perinuclear region, (**7**) DNA must cross the nuclear envelope to be finally expressed and (**8**) yield proteins released into the cytoplasm.

Early endosomes represent the organelles where the primary endocytic vesicles of almost any nature deliver their content and membranes.[51] Given our demonstration that most DNA aggregates are endocytosed, we expected to observe DNA in Rab5 vesicles and indeed the sum of the correlation and colocalization percentages indicated that about 70% of internalized DNA is located in such structures. This confirms that DNA internalization mainly occurs via endocytosis and that the next predominant step of delivery is its passage through early endosomes. Some primary vesicles such as GEEC ones can be found in Rab5-negative early endosomes.[59] It is therefore possible that some of the DNA is present in such organelles.

The content of early endosomes can proceed via several routes, *e.g.*, it can be recycled directly to the plasma membrane or via the recycling endosomes[60] and it can undergo further trafficking in endosomal vesicles by passing through maturating and late endosomes. Alternatively, it can also be transported to the Golgi.[59] Our experiments indicate that a substantial fraction of internalized DNA (50%) is directed to the recycling endosomes. However, Rab11 can be found in Rab5 organelles,[58] which suggests that some of the DNA colocalizing with Rab11 can still reside in early endosomes. Recycling is used to relocalize, for example, receptors to the plasma membrane. Since during its electrophoresis, DNA is inserted into the plasma membrane, the cell machinery may sort DNA in the same way as for a receptor.

The correlation and colocalization of DNA with Rab9 showed that it is further trafficked into late endosomes. Rab9 also characterizes vesicles shuttling between late endosomes and Golgi or lysosomes. We found that ~30% of DNA coincided with Rab9. However, it should be considered that the data were recorded between 15 minutes and 1.5 hours after gene electrotransfer. It is possible that observations taken at a later time would reveal elevated presence of DNA in Rab9 structures. The fact that we found much higher amounts of DNA colocalizing with Lamp1 may also reflect that more than 30% of DNA might pass by late endosomes. The fusion of a late endosome with a lysosome generates a transient hybrid organelle, the endolysosome, in which active degradation already takes place.[58] Endolysosomes contain both Rab9 and Lamp1 proteins in their membranes while lysosomes contain only Lamp1. Large amounts of DNA localized to (endo)lysosomes, as from 1 to 2 hours after gene electrotransfer ~60% of DNA colocalized with Lamp1. This means that, as is the case for other nonviral methods, plasmids are lost in significant quantities in lysosomes. Several reviews mention the possibility of vesicles shuttling between lysosomes and the Golgi or the ER, which would give the endocytosed DNA a last chance to escape degradation.[51,58]

We have found that the majority of internalized DNA aggregates undergo endosomal trafficking. During the maturation process, endosomes move toward the perinuclear space along microtubules. Moreover, Rab proteins are believed to act as receptors for motor proteins either via a direct interaction or through intermediary proteins.[61] We have recently shown that DNA aggregates are actively transported along actin filaments and microtubules.[21] Electrotransferred DNA exhibited the typical motion of endosomes or other cargo with intermittent phases of active transport and diffusion. Endosomal trafficking of DNA allows it to travel through the cytoplasm in an efficient manner and to remain relatively well protected from cytosolic enzymes. However, if DNA does not escape from endosomes before reaching lysosomes, it is probably lost for gene expression. DNA in recycling endosomes is also most likely lost for the purposes of transfection. The development of strategies fostering the efficient escape of DNA from late endosomes and lysosomes, therefore, appears to be an important step in the improvement of gene-transfer methods based on electroporation.

Conclusion

After electroporation, the transport process of DNA from the plasma membrane to the nuclear envelop appears to be very similar to that observed for other nonviral and viral-based delivery methods (**Figure 7**). DNA aggregates, which are rapidly formed at the plasma membrane, are endocytosed by numerous endocytic pathways (**Figure 7**, steps 1–4). Since many different endocytic inhibitors decrease DNA expression, endocytosis in general appears to be crucial for gene expression after electrotransfer. Correlation and colocalization of DNA with various endosomal markers clearly shows that electrotransferred DNA is routed through the different endosomal compartments (**Figure 7**, step 5). An important step for future work is the investigation of putative endosomal escape (**Figure 7**, step 6), which is critical for successful gene expression.

Materials and methods

Cell culture. The wild-type (Toronto strain) CHO were grown in Eagle's minimum essential medium supplemented as described in Ref. 21. Cells were subcultured every 2–3 days and incubated at 37 °C in a humidified atmosphere with a 5% CO_2 incubator.

Plasmids. pEGFP-C1 plasmids (Clonetech, Palo Alto, CA) were prepared from transformed DH5α *Escherichia coli* using the Maxiprep DNA purification system according to manufacturer instructions (Qiagen, Chatsworth, CA). For microscopy experiments, the plasmids were covalently stained with Cy5 or Cy3 dye using the Label IT Nucleic Acid Labeling Kit (Mirus, Madison, WI) according to manufacturer instructions. The plasmid constructs pEGFP-Rab5, pEGFP-Rab9, pEGFP-Rab11, and pEGFP-Lamp1 were kindly gifted by Prof. Dr. C. Hauck (University of Konstanz, Germany) and prepared as described above.

Pharmacological inhibitors. Incubations were performed for 1 hour prior to the application of the electric field at 37 °C. CPZ (1–50 µmol/l) and MDC (50–200 µmol/l) inhibit clathrin-mediated endocytosis (resp. Enzo Life Sciences, Farmingdale, NY and Sigma-Aldrich, St-Louis, MO). Gen (50–200 µmol/l) and Fil (0.1–2.5 µmol/l) affect raft/caveolin-mediated endocytosis (resp. Enzo Life Sciences and Sigma-Aldrich). EIPA (10–100 µmol/l) and Wort (0.02–0.5 µmol/l) alter macropinocytosis (Enzo Life Sciences). MβCD (1–5 µmol/l), as a cholesterol sequester, can inhibit clathrin-, raft/caveolin-, or any other cholesterol dependent-mediated endocytosis

(Sigma-Aldrich). These concentrations were chosen based on cell viabilities (higher than 60%).

Endocytic markers. Alexa Fluor 647-Tf (Molecular Probes-InvitroGen, Carlsbad, CA) was used to test for the clathrin-mediated endocytosis pathway, Alexa Fluor 647-CTB (Molecular Probes-InvitroGen) to test for the caveolin/raft-mediated endocytosis pathway and rhodamine-(70-kDa)-dextran (Molecular Probes-InvitroGen), to quantify fluid-phase endocytosis. 24 hours prior to electroporation, 2×10^5 cells were cultured on Lab-Tek II slides (Nunc, Roskilde, Denmark). The cells were incubated at 4 °C for 30 minutes to inhibit any endocytic process. Subsequently, the cells were pulsed in 300 µl pulsation buffer containing 1 µg Cy3- or Cy5-labeled DNA using 10-mm length plate electrodes. Five minutes after electroporation, the pulsation buffer was removed and ice-cold culture medium containing the endocytic marker (50 µg/ml Tf or 1 µg/ml CTB or 500 µg/ml dextran) was added. The cells were incubated at 4 °C for another 30 minutes to allow for the endocytic marker to interact with the plasma membrane without endocytosis taking place. Afterward, the cells were incubated for 15 min at 37 °C to induce endocytosis.

Electroporation procedures. Electric fields were applied with the ElectroCell S20 electropulsator (βtech, Toulouse, France) delivering square-wave electric pulses. The pulse parameters: amplitude, duration, number, and frequency were controlled independently and monitored using an oscilloscope (HM1507-3, HAMEG GmbH, Frankfurt, Germany). For DNA electrotransfer into CHO cells, the optimal parameters are 10 pulses of 5 ms at 1 Hz frequency with electric field strengths between 0.4 and 0.8 kV/cm.[10] Two stainless-steel electrodes (parallel plate electrodes of 10-mm length), with an inter-electrode distance of 5 or 10 mm, were used respectively for the electroporation of suspended or adherent cells. Electric fields were applied in a pulsation buffer (10-mmol/l K_2HPO_4/KH_2PO_4, pH 7.4, 1-mmol/l $MgCl_2$, 250-mmol/l sucrose) in which cells were kept for few minutes after the application of the electric field to allow for membrane resealing. For gene expression experiments, 3.5×10^4 cells were cultured on coverslips (Thermanox, Nunc, Roskilde, Denmark) deposed in 24-well plates (Corning Inc., Corning, NY) and pulsed in the presence of 2 µg of pEGFP-C1 in 200-µl pulsation buffer. The electric field strength was 0.4 kV/cm.[10] For microscopy experiments, 2.5×10^5 cells were cultured on 22×22-mm chambered coverglass (Lab-Tek II, Nunc, Roskilde, Denmark) and pulsed at 0.4 kV/cm in the presence of 1 µg Cy5- or Cy3-labeled pEGFP-C1 in 300-µl pulsation buffer. For the dual-color experiments, cells were transfected 24 hours beforehand in suspension with the EGFP-tagged proteins (10^6 cells in 100-µl pulsation buffer containing 2-µg plasmid). The strength of the electric field was 0.6 kV/cm.

Gene expression procedure. 3.5×10^4 cells were deposed as a spread drop of 50 µl on a 13-mm diameter coverslip (Thermanox) that matched the size of the electrodes (10×10 mm) and was laid down in a 24-well plate. After cell adhesion (20 minutes at 37 °C), 1 ml culture medium was added and the cells were cultured for 24 hours. Drug incubations were performed 1 hour before the application of the electric field at 37 °C. Electric fields were applied as described in the electroporation procedures section. After 24 hours, the samples were analyzed by flow cytometry (FACScan, Becton Dickinson, Franklin Lakes, NJ) via the FL1 channel (510 nm $\leq \lambda_{em} \leq$ 540 nm) to evaluate both the percentage of EGFP fluorescent cells (transfection efficiency) and the mean level of fluorescence associated with them (transfection level). All values were normalized in relation to the control cells, which were transfected but not treated with drugs. Only viable cell populations were analyzed to not take into account the cell mortality due to the drug treatment and the application of the electric field.

Fluorescence microscopy. Two solid state lasers, 491- and 561-nm wavelength, (Cobolt Calypso 491 nm and Cobolt Jive 561 nm, 75 mW, Cobolt AB, Stockholm, Sweden) and a 658-nm diode laser (HL6535MG 658 nm, 90 mW Hitachi, Thorlabs, Newton, NJ) were used as light sources. Laser beams were first coupled into a multimode fiber (0.22±0.02 NA, Optronis GmbH, Kehl, Germany), and then into an 100×/1.4 NA oil immersion objective (HCX PL APO, Leica Microsystems GmbH, Wetzlar, Germany) mounted on a Leica DMI 6000B inverted microscope equipped with a heating stage connected to a temperature controller set to 37 °C. Dual band dichroic mirrors were used according to the desired wavelength (z 488/658, z 561/660, Dual Line Beamsplitter, Semrock, Rochester, NY). A fast switching filter wheel (motorized fast-change filter wheel, Thorlabs) containing the emission filters was placed between the microscope and the cooled EMCCD (electron multiplier CCD) camera (Andor iXON, Andor Technology PLC, Belfast, Ireland). The fluorescence emitted from blue labels (*e.g.*, EGFP) was selected using a band-pass filter (BrightLine HC 538/25, Semrock). The fluorescence emitted from the green labels (*e.g.*, Cy3, rhodamine) was selected using a long-pass filter (Raman emitter RU 568, Semrock) or a band-pass filter (BrightLine HC 593/40, Semrock). The fluorescence emitted from the red labels (Cy5, Alexafluor 647) was selected using a long-pass filter (Raman emitter RU 664, Semrock) or a band-pass filter (BrightLine HC 694/40, Semrock). Each pixel represented 54 nm of the sample. Time series of 200 frames for each color were recorded with 100 ms exposure time and with 100 ms delay to switch the filters placed in the motorized wheel.

Colocalization analysis. Particle tracking was performed using Imaris 7.2 software (Bitplane AG, Zurich, Switzerland). The positions were determined for each frame of the movie stack via the "spots objects" option and the trajectory paths were constructed using the autoregressive motion algorithm. Dynamic colocalization is defined as correlation between the trajectory positions. The trajectories were analyzed with a previously established dynamic colocalization algorithm.[25] The Pearson correlation coefficient was calculated for the each position coordinates of the trajectories in both channels, in both the *x*- and *y* directions. If the value exceeded a certain threshold (0.45), in both the *x*- and *y* directions, the two trajectories were considered to be correlated. Uncorrelated trajectories were then analyzed based on static colocalization. If the standard deviation of their position coordinates was below 500 nm, in both the *x*- and *y* directions, the center of each trajectory was determined as the mean position. If the distance between the center of the first channel trajectory and that of the second channel trajectory was below 250 nm, in both the directions, the corresponding trajectories were considered to be colocalized.

Statistical test. Error bars represent the standard error of the mean. The statistical significance of differences in gene expression efficiency (percentage of transfected cells and their mean fluorescence level) between the control and drug treated cells was evaluated by the nonparametric Mann–Whitney–Wilcoxon test. The degree of significance is given with these following labels: $^{*}P < 0.05$; $^{**}P < 0.01$; $^{***}P < 0.001$.

Supplementary material

Figure S1. Colocalization between 70-kDa dextran and transferrin or cholera toxin B.

Acknowledgments We acknowledge financial support from the Deutscher Akademischer Austauschdienst (DAAD), the Ministère des Affaires Etrangères (MAE) and the Ministère de l'Enseignement Supérieur et de la Recherche (MESR) (program PHC PROCOPE 2010–2011). This research was conducted in the scope of the EBAM European Associated Laboratory (LEA EBAM) and COST TD 1104. Financial support by the Ghent University Special Research Fund and the Fund for Scientific Research Flanders (FWO, Belgium) is acknowledged by Kevin Braeckmans with gratitude. Part of this work was funded by the Deutsche Forschungsgemeinschaft (DFG), SFB 969, TP B08 and by the French Agency for National Research (ANR Astrid PIERGEN, ANR-12-ASTR-0039-01).

1. Marty, M, Sersa, G, Garbay, JR, Gehl, J, Collins, CG, Snoj, M, *et al.* (2006). Electrochemotherapy—an easy, highly effective and safe treatment of cutaneous and subcutaneous metastases: results of ESOPE (European Standard Operating Procedures of Electrochemotherapy) study. *EJC Suppl* **4**: 3–13.
2. Yarmush, ML, Golberg, A, Serša, G, Kotnik, T and Miklavčič, D (2014). Electroporation-based technologies for medicine: principles, applications, and challenges. *Annu Rev Biomed Eng* **16**: 295–320.
3. Gothelf, A, Mir, LM and Gehl, J (2003). Electrochemotherapy: results of cancer treatment using enhanced delivery of bleomycin by electroporation. *Cancer Treat Rev* **29**: 371–387.
4. Daud, AI, DeConti, RC, Andrews, S, Urbas, P, Riker, AI, Sondak, VK *et al.* (2008). Phase I trial of interleukin-12 plasmid electroporation in patients with metastatic melanoma. *J Clin Oncol* **26**: 5896–5903.
5. Low, L, Mander, A, McCann, K, Dearnaley, D, Tjelle, T, Mathiesen, I *et al.* (2009). DNA vaccination with electroporation induces increased antibody responses in patients with prostate cancer. *Hum Gene Ther* **20**: 1269–1278.
6. Gothelf, A and Gehl, J (2012). What you always needed to know about electroporation based DNA vaccines. *Hum Vaccin Immunother* **8**: 1694–1702.
7. Young, JL and Dean, DA (2015). Electroporation-mediated gene delivery. *Adv Genet* **89**: 49–88.
8. Vandermeulen, G, Staes, E, Vanderhaeghen, ML, Bureau, MF, Scherman, D and Préat, V (2007). Optimisation of intradermal DNA electrotransfer for immunisation. *J Control Release* **124**: 81–87.
9. Krassowska, W and Filev, PD (2007). Modeling electroporation in a single cell. *Biophys J* **92**: 404–417.
10. Golzio, M, Teissie, J and Rols, MP (2002). Direct visualization at the single-cell level of electrically mediated gene delivery. *Proc Natl Acad Sci USA* **99**: 1292–1297.
11. Klenchin, VA, Sukharev, SI, Serov, SM, Chernomordik, LV and Chizmadzhev YuA (1991). Electrically induced DNA uptake by cells is a fast process involving DNA electrophoresis. *Biophys J* **60**: 804–811.
12. Glogauer, M, Lee, W and McCulloch, CA (1993). Induced endocytosis in human fibroblasts by electrical fields. *Exp Cell Res* **208**: 232–240.
13. Rols, MP, Femenia, P and Teissie, J (1995). Long-lived macropinocytosis takes place in electropermeabilized mammalian cells. *Biochem Biophys Res Commun* **208**: 26–35.
14. Antov, Y, Barbul, A and Korenstein, R (2004). Electroendocytosis: stimulation of adsorptive and fluid-phase uptake by pulsed low electric fields. *Exp Cell Res* **297**: 348–362.
15. Antov, Y, Barbul, A, Mantsur, H and Korenstein, R (2005). Electroendocytosis: exposure of cells to pulsed low electric fields enhances adsorption and uptake of macromolecules. *Biophys J* **88**: 2206–2223.
16. Rosazza, C, Phez, E, Escoffre, JM, Cézanne, L, Zumbusch, A and Rols, MP (2012). Cholesterol implications in plasmid DNA electrotransfer: evidence for the involvement of endocytotic pathways. *Int J Pharm* **423**: 134–143.
17. Wu, M and Yuan, F (2011). Membrane binding of plasmid DNA and endocytic pathways are involved in electrotransfection of mammalian cells. *PLoS One* **6**: e20923.
18. Markelc, B, Skvarca, E, Dolinsek, T, Kloboves, VP, Coer, A, Sersa, G *et al.* (2015). Inhibitor of endocytosis impairs gene electrotransfer to mouse muscle in vivo. *Bioelectrochemistry* **103**: 111–119.
19. Rosazza, C, Escoffre, JM, Zumbusch, A and Rols, MP (2011). The actin cytoskeleton has an active role in the electrotransfer of plasmid DNA in mammalian cells. *Mol Ther* **19**: 913–921.
20. Bamford, RA, Zhao, ZY, Hotchin, NA, Styles, IB, Nash, GB, Tucker, JH *et al.* (2014). Electroporation and microinjection successfully deliver single-stranded and duplex DNA into live cells as detected by FRET measurements. *PLoS One* **9**: e95097.
21. Rosazza, C, Buntz, A, Rieß, T, Wöll, D, Zumbusch, A and Rols, MP (2013). Intracellular tracking of single-plasmid DNA particles after delivery by electroporation. *Mol Ther* **21**: 2217–2226.
22. Ivanov, AI (2008). Pharmacological inhibition of endocytic pathways: is it specific enough to be useful? *Methods Mol Biol* **440**: 15–33.
23. Bolte, S and Cordelières, FP (2006). A guided tour into subcellular colocalization analysis in light microscopy. *J Microsc* **224**: 213–232.
24. Lachmanovich, E, Shvartsman, DE, Malka, Y, Botvin, C, Henis, YI and Weiss, AM (2003). Co-localization analysis of complex formation among membrane proteins by computerized fluorescence microscopy: application to immunofluorescence co-patching studies. *J Microsc* **212**: 122–131.
25. Vercauteren, D, Deschout, H, Remaut, K, Engbersen, JF, Jones, AT, Demeester, J *et al.* (2011). Dynamic colocalization microscopy to characterize intracellular trafficking of nanomedicines. *ACS Nano* **5**: 7874–7884.
26. Boisvert, M and Tijssen, P (2012). Endocytosis of non-enveloped DNA viruses. In: B. Ceresa (ed.). *Molecular Regulation of Endocytosis.* Rijeka, Croatia: InTech. ISBN: 978-953-51-0662-3.
27. Tulapurkar, ME, Schäfer, R, Hanck, T, Flores, RV, Weisman, GA, González, FA *et al.* (2005). Endocytosis mechanism of P2Y2 nucleotide receptor tagged with green fluorescent protein: clathrin and actin cytoskeleton dependence. *Cell Mol Life Sci* **62**: 1388–1399.
28. Yao, D, Ehrlich, M, Henis, YI and Leof, EB (2002). Transforming growth factor-beta receptors interact with AP2 by direct binding to beta2 subunit. *Mol Biol Cell* **13**: 4001–4012.
29. Inal, J, Miot, S and Schifferli, JA (2005). The complement inhibitor, CRIT, undergoes clathrin-dependent endocytosis. *Exp Cell Res* **310**: 54–65.
30. Rodal, SK, Skretting, G, Garred, O, Vilhardt, F, van Deurs, B and Sandvig, K (1999). Extraction of cholesterol with methyl-beta-cyclodextrin perturbs formation of clathrin-coated endocytic vesicles. *Mol Biol Cell* **10**: 961–974.
31. Subtil, A, Gaidarov, I, Kobylarz, K, Lampson, MA, Keen, JH and McGraw, TE (1999). Acute cholesterol depletion inhibits clathrin-coated pit budding. *Proc Natl Acad Sci USA* **96**: 6775–6780.
32. Zuhorn, IS, Kalicharan, R and Hoekstra, D (2002). Lipoplex-mediated transfection of mammalian cells occurs through the cholesterol-dependent clathrin-mediated pathway of endocytosis. *J Biol Chem* **277**: 18021–18028.
33. Qualmann, B and Kessels, MM (2002). Endocytosis and the cytoskeleton. *Int Rev Cytol* **220**: 93–144.
34. Lajoie, P and Nabi, IR (2010). Lipid rafts, caveolae, and their endocytosis. *Int Rev Cell Mol Biol* **282**: 135–163.
35. Doherty, GJ and McMahon, HT (2009). Mechanisms of endocytosis. *Annu Rev Biochem* **78**: 857–902.
36. Kabouridis, PS, Janzen, J, Magee, AL and Ley, SC (2000). Cholesterol depletion disrupts lipid rafts and modulates the activity of multiple signaling pathways in T lymphocytes. *Eur J Immunol* **30**: 954–963.
37. Sahay, G, Alakhova, DY and Kabanov, AV (2010). Endocytosis of nanomedicines. *J Control Release* **145**: 182–195.
38. Pelkmans, L, Püntener, D and Helenius, A (2002). Local actin polymerization and dynamin recruitment in SV40-induced internalization of caveolae. *Science* **296**: 535–539.
39. Schnitzer, JE, Oh, P, Pinney, E and Allard, J (1994). Filipin-sensitive caveolae-mediated transport in endothelium: reduced transcytosis, scavenger endocytosis, and capillary permeability of select macromolecules. *J Cell Biol* **127**: 1217–1232.
40. Nonnenmacher, M and Weber, T (2011). Adeno-associated virus 2 infection requires endocytosis through the CLIC/GEEC pathway. *Cell Host Microbe* **10**: 563–576.
41. Henley, JR, Krueger, EW, Oswald, BJ and McNiven, MA (1998). Dynamin-mediated internalization of caveolae. *J Cell Biol* **141**: 85–99.

42. Oh, P, McIntosh, DP and Schnitzer, JE (1998). Dynamin at the neck of caveolae mediates their budding to form transport vesicles by GTP-driven fission from the plasma membrane of endothelium. *J Cell Biol* **141**: 101–114.
43. Parton, RG, Joggerst, B and Simons, K (1994). Regulated internalization of caveolae. *J Cell Biol* **127**: 1199–1215.
44. Lajoie, P, Goetz, JG, Dennis, JW and Nabi, IR (2009). Lattices, rafts, and scaffolds: domain regulation of receptor signaling at the plasma membrane. *J Cell Biol* **185**: 381–385.
45. Lajoie, P and Nabi, IR (2007). Regulation of raft-dependent endocytosis. *J Cell Mol Med* **11**: 644–653.
46. Kirkham, M and Parton, RG (2005). Clathrin-independent endocytosis: new insights into caveolae and non-caveolar lipid raft carriers. *Biochim Biophys Acta* **1745**: 273–286.
47. Lajoie, P, Kojic, LD, Nim, S, Li, L, Dennis, JW and Nabi, IR (2009). Caveolin-1 regulation of dynamin-dependent, raft-mediated endocytosis of cholera toxin-B sub-unit occurs independently of caveolae. *J Cell Mol Med* **13**: 3218–3225.
48. Glebov, OO, Bright, NA and Nichols, BJ (2006). Flotillin-1 defines a clathrin-independent endocytic pathway in mammalian cells. *Nat Cell Biol* **8**: 46–54.
49. Lambert, H, Pankov, R, Gauthier, J and Hancock, R (1990). Electroporation-mediated uptake of proteins into mammalian cells. *Biochem Cell Biol* **68**: 729–734.
50. Zimmermann, U, Schnettler, R, Klöck, G, Watzka, H, Donath, E and Glaser, RW (1990). Mechanisms of electrostimulated uptake of macromolecules into living cells. *Naturwissenschaften* **77**: 543–545.
51. Mercer, J, Schelhaas, M and Helenius, A (2010). Virus entry by endocytosis. *Annu Rev Biochem* **79**: 803–833.
52. West, MA, Bretscher, MS and Watts, C (1989). Distinct endocytotic pathways in epidermal growth factor-stimulated human carcinoma A431 cells. *J Cell Biol* **109**: 2731–2739.
53. Dowrick, P, Kenworthy, P, McCann, B and Warn, R (1993). Circular ruffle formation and closure lead to macropinocytosis in hepatocyte growth factor/scatter factor-treated cells. *Eur J Cell Biol* **61**: 44–53.
54. Araki, N, Johnson, MT and Swanson, JA (1996). A role for phosphoinositide 3-kinase in the completion of macropinocytosis and phagocytosis by macrophages. *J Cell Biol* **135**: 1249–1260.
55. Mercer, J and Helenius, A (2009). Virus entry by macropinocytosis. *Nat Cell Biol* **11**: 510–520.
56. Grimmer, S, van Deurs, B and Sandvig, K (2002). Membrane ruffling and macropinocytosis in A431 cells require cholesterol. *J Cell Sci* **115**: 2953–2962.
57. Rajendran, L, Knölker, HJ and Simons, K (2010). Subcellular targeting strategies for drug design and delivery. *Nat Rev Drug Discov* **9**: 29–42.
58. Huotari, J and Helenius, A (2011). Endosome maturation. *EMBO J* **30**: 3481–3500.
59. Perret, E, Lakkaraju, A, Deborde, S, Schreiner, R and Rodriguez-Boulan, E (2005). Evolving endosomes: how many varieties and why? *Curr Opin Cell Biol* **17**: 423–434.
60. Maxfield, FR and McGraw, TE (2004). Endocytic recycling. *Nat Rev Mol Cell Biol* **5**: 121–132.
61. Murray, JW and Wolkoff, AW (2003). Roles of the cytoskeleton and motor proteins in endocytic sorting. *Adv Drug Deliv Rev* **55**: 1385–1403.

Supplementary Information accompanies this paper on the Molecular Therapy–Nucleic Acids website (http://www.nature.com/mtna)